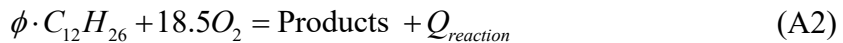


Appendix A. Reduced “flame”-sheet model

Keyes’ approach assumed that the flame proceeds with one step, and infinitely fast kinetics for use as an initial guess for the detailed opposed flow flame model. Therefore, the Shvab-Zeldovich coupling functions can be used. Keyes et al. solved the flame sheet model by considering the following governing equations:

$$\begin{aligned}
 \frac{dV}{dy} + \alpha(1 + \alpha)\rho f' &= 0 \\
 \frac{d}{dy} \left(\mu \frac{df'}{dy} \right) - V \frac{df'}{dy} + a(\rho_\infty - \rho(f')^2) &= 0 \\
 \frac{d}{dy} \left(\rho D_X \frac{dY_X}{dy} \right) - V \frac{dY_X}{dy} + W_X v_X \dot{w}_X &= 0, \quad X = F, O, P, \text{ or } N \\
 \frac{d}{dy} \left(\lambda \frac{dT}{dy} \right) - V c_p \frac{dT}{dy} + (W_F v_F h_F + W_O v_O h_O - W_P v_P h_P) \dot{w} &= 0
 \end{aligned} \tag{A1}$$

Where α is a geometric factor with a value of 0 for Cartesian coordinates, a is the strain rate, ρ is the mass density; v is the velocity; V is defined as $V = \rho \cdot v$; f' is the scaled axial velocity defined as u/U , which is also related to the derivative of a modified stream function; μ is the viscosity; D is the diffusion coefficient and F, O, P, N stand for fuel, oxidizer, product, and nitrogen, respectively; Y is the mass fraction; W the molecular weight, v the stoichiometric coefficient, \dot{w} rate of progress of the reaction as defined in [1] indicating the global consuming rate of fuel and oxidizer; λ the thermal conductivity; c_p the constant pressure heat capacity; T the temperature, and h the specific enthalpy. In this work, n-dodecane is the fuel and oxygen is the oxidizer. The unity Lewis Number assumption was used throughout as in [1]. Using the flame sheet approach, fuel and oxidizer cannot co-exist in the reaction zone. To determine reactant product concentrations and reaction heat from the reforming process, our reactor numerical model adopted a similar one-step reaction to Keyes:



“Products” was defined as the collection of all reforming products as a single species. The physical properties of “Products” were calculated from the weighted averages of all reforming products to predict overall reactor features like temperature distribution and local stoichiometry. Since reactor temperatures were estimated to be low (< 500 °C), our model assumes that all reactions occur on the catalytic mesh acting as the flame sheet. This is an approximation since intermediate products from the mesh may react with fuel vapor or air. However, the flame sheet approximation is deemed more appropriate here than for a high temperature flame reactor since the reaction rates at the mesh are assumed to be significantly higher than in the gas phase due to its catalytic activity. The flame sheet approximation is deemed suitable for the purposes of comparing temperature trends to experimental data. A single-zone constant pressure, constant enthalpy thermodynamic equilibrium calculation was performed using Cantera [2] with thermal parameters given in [3] to give a realistic reaction heat comparing to complete combustion assumptions. Since there was not an appropriate n-dodecane catalytic surface reaction mechanism available from the literature, the model considered only n-dodecane gas phase reactions and could not distinguish between different catalysts. Therefore, the same model was used for both platinum catalyst and rhodium catalysts.

In Keyes’ development, the location of the flame front was calculated by finding the location where local equivalence ratio equals 1, as indicated in Eq. (3.29) in Keyes’ paper:

$$S(y_f) = Y_{O_{\infty}} / (Y_{O_{\infty}} + W_o v_o / W_F v_F \cdot Y_{F-\infty}) \quad (\text{A3})$$

Where S is the conserved scalar as defined in [1], $Y_{O_{\infty}}$ is the mass fraction of oxygen at the air inlet, $Y_{F-\infty}$ is the mass fraction of fuel at the diesel pool surface. In Keyes’ model, all variables in the right hand side of Eq. (A2) are known and S was calculated to find the flame location. In this work, the location of the flame sheet is predetermined by the location of the catalytic mesh, and $v_F(\phi_g)$ is unknown since the ϕ_{mesh} is no longer fixed at 1.0. Therefore, Eq. (A3) is rearranged into:

$$v_F(\phi) = \frac{w_o v_o Y_{F-\infty}}{w_f Y_{o\infty} (1/S(y_f) - 1)} \quad (\text{A3a})$$

and solve Eq. (A3a) for v_F instead of S in each iteration in our revised model to reflect non-stoichiometric reactions.

The network method of radiation heat transfer [4] is adopted to calculate the heat transferred to the fuel pool and heat loss from the mesh. The reactor was considered to be a three-surface system including the mesh surface (assumed it is a disk), fuel surface, and ambient air. When the distance from the mesh to the fuel pool changed, view factors of the system also changed and the net heat flux could be found by using Kirchhoff Circuit Laws. In this work, the view factor from the mesh to the fuel is given by:

$$A_{SF} = \frac{1}{2} \{S - [S^2 - 4(\frac{r_F}{r_S})^2]^{1/2}\}, \text{ where } S = 1 + \frac{1 + R_F^2}{R_S^2}, R_F = r_F / d, R_S = r_S / d \quad (\text{A4})$$

Where r_F and r_S are radius of the fuel pool and the mesh, respectively, and d is the distance from the mesh to the fuel pool. In this work, it was determined that the emissivity of the catalytic mesh in separate experiments by heating it to various temperatures then placing it in different axial locations above the pool and recording fuel evaporation rate. Mesh and pool emissivity were then solved in a least-square sense with more than 10 equations/conditions with parallel plates radiative heat transfer assumptions. The procedure was repeated multiple times and averaged emissivity was obtained. The emissivity of fuel and mesh were found to be 0.99 and 0.45, respectively, which are within the typical range from literature. To account for the heat loss from the mesh in the model, a radiation term was added in the energy equation as shown below [5]:

$$\frac{d}{dy} \left(\lambda \frac{dT}{dy} \right) - \rho v c_p \frac{dT}{dy} + (Q_{reaction} - Q_{rad}) \dot{w} = 0 \quad (\text{A5})$$

Where λ is thermal conductivity, c_p is the specific heat of gas, ρ is density, v is the transverse component of velocity, Q_{rad} is heat loss from radiation, and \dot{w} is the rate of fuel/air consumption. Lastly, since the

exit Reynolds numbers are relatively small, a buoyancy term was added in the momentum equation as indicated by [6]. The remaining calculation steps were similar to those in Keyes's model. Other thermal and transport properties of n-dodecane were selected from [7]. The flow boundary conditions for numerical modeling were chosen based on experiment measurements and temperature boundary conditions were taken from centerline thermocouple measurements near the air inlet and fuel pool. Although the catalytic mesh is expected to alter the local u component velocity since it acts as a flow restriction, the 1D flame sheet model was assumed to accurately predict temperature along the centerline of the reactor since $u = 0$ at the centerline.

The flame sheet modeling results show that dry species concentration on the fuel side of the catalytic mesh (0 – 3 mm for Condition 1 and 0 – 4 mm for Condition 2) did not vary as a function of y . The concentration for each species held a constant value. This phenomenon was well explained by the flame sheet model. On the fuel side, the species concentration of the product can be expressed as:

$$Y_p(y) = \frac{C_p w_p v_p}{Q w_f v_f} [T(y) - T_\infty + T_\infty S(y) - T_\infty S(y)] \quad (\text{A6})$$

And fuel concentration can be written as:

$$Y_f(y) = Y_{f-\infty} - \frac{C_p}{Q} [T(y) - T_\infty + T_\infty S(y) - T_\infty S(y)] \quad (\text{A7})$$

Note that $Y_{f-\infty} = 1$ and therefore it is obvious that:

$$\frac{Y_p(y)}{1 - Y_f(y)} = \frac{\frac{C_p w_p v_p}{Q w_f v_f} [T(y) - T_\infty + T_\infty S(y) - T_\infty S(y)]}{\frac{C_p}{Q} [T(y) - T_\infty + T_\infty S(y) - T_\infty S(y)]} = \frac{w_p v_p}{w_f v_f} = \text{constant} \quad (\text{A8})$$

Note that water vapor species concentration is proportional to total reaction product concentration according to the flame sheet model assumption.

Reference

- [1] D. Keyes, M. Smooke, Flame sheet starting estimates for counterflow diffusion flame problems, *Journal of Computational Physics* 73 (1987) 267-288.
- [2] H.K.M. David G. Goodwin, and Raymond L. Speth. , Cantera: An object- oriented software toolkit for chemical kinetics, thermodynamics, and transport processes. <http://www.cantera.org>, doi:doi:10.5281/zenodo.170284 doi:|.
- [3] Z. Luo, S. Som, S.M. Sarathy, M. Plomer, W.J. Pitz, D.E. Longman, T. Lu, Development and validation of an n-dodecane skeletal mechanism for spray combustion applications, *Combustion theory and modelling* 18 (2014) 187-203.
- [4] A.Ç. Yunus, J.G. Afshin, *Heat and Mass Transfer*, McGrawHill, New York, (2007).
- [5] X. Zhu, J. Gore, Radiation effects on combustion and pollutant emissions of high-pressure opposed flow methane/air diffusion flames, *Combustion and Flame* 141 (2005) 118-130.
- [6] U. Niemann, K. Seshadri, F.A. Williams, Accuracies of laminar counterflow flame experiments, *Combustion and Flame* 162 (2015) 1540-1549.
- [7] C.L. Yaws, *Yaws' transport properties of chemicals and hydrocarbons*, Knovel New York, NY2010.